Publishing Excellence
Inspiring Progress
ARISTON PUBLICATIONS
ChemSci Advances
ISSN: 2997-9587 https://aristonpubs.com/journal/chemsci-advances https://doi.org/10.69626/csa.2026.0151

REVIEW ARTICLE

Photocatalytic Degradation of Congo Red: Catalysts, Mechanisms, and Process Parameters

Mahendra Ramdas Thomare[1*], Vishnu A. Adole[2], Kailas H. Kapadnis[2]

ABSTRACT: Congo red, a toxic anionic azo dye extensively used in textile, paper, and leather industries, poses serious environmental and health risks owing to its recalcitrant nature and carcinogenic potential. This review examines recent progress in photocatalytic degradation technologies for Congo red removal from aqueous solutions. The analysis includes diverse photocatalyst systems such as metal oxides (TiO_2, ZnO, Y_2O_3, NiO), ferrites ($MgFe_2O_4$, $MnFe_2O_4$, AFe_2O_4), nanocomposites, and heterostructures. Reported degradation efficiencies vary widely from 24% to 98%, depending on catalyst composition, synthesis route, and operational conditions. Visible-light-active photocatalysts, particularly doped metal oxides and ferrite-based materials with bandgap energies between 2.14 and 2.19 eV, consistently outperform conventional UV-activated catalysts. Hydroxyl radicals and superoxide anions are identified as the dominant reactive oxygen species driving Congo red mineralization. Cerium-substituted Mn–Zn ferrites and alkaline earth ferrites emerge as especially promising systems, achieving degradation efficiencies of 92–97% under visible light irradiation while offering the added benefit of magnetic recoverability. Heterostructure designs, including TiO_2–graphene oxide and CS-BiOCl/ZnO nanocomposites, demonstrate that rational material engineering can overcome the limitations of single-component systems. Despite these advances, challenges related to charge carrier recombination, long-term stability, visible light utilization, and scalability persist. Future research should prioritize the development of cost-effective, magnetically recoverable, and highly efficient photocatalysts, along with pilot-scale demonstrations and comprehensive toxicity assessments, to enable practical wastewater treatment applications.

Keywords: Congo Red, Photocatalysis, Ferrites, Reactive Oxygen Species, Wastewater Treatment

Received: 15 May 2026; Revised: 13 July 2026; Accepted: 24 July 2026; Published Online: 15 August 2026

1. INTRODUCTION

The rapid expansion of textile, paper, and dyeing industries has resulted in the discharge of large volumes of dye-contaminated wastewater into aquatic ecosystems, creating severe environmental challenges that threaten both ecological balance and human health. Among the various synthetic dyes, Congo red ($C_{32}H_{22}N_6Na_2O_6S_2$) is a benzidine-based anionic azo dye extensively used for coloring textiles, paper, and leather products. Its complex aromatic structure, characterized by azo bonds (–N=N–), renders it highly stable and resistant to conventional biological and chemical treatment methods. The presence of Congo red in water bodies not only impairs aesthetic quality but also blocks light penetration, thereby inhibiting photosynthesis and disrupting aquatic ecosystems. More critically, Congo red and its degradation intermediates exhibit carcinogenic and mutagenic properties, posing serious risks to aquatic organisms and human populations exposed through contaminated water sources [1]. The cleavage of its azo groups can release benzidine, a well-recognized carcinogen, which has prompted restrictions on the use of this dye in several applications [2].

Traditional wastewater treatment methods, including coagulation-flocculation, adsorption, and biological treatment, often prove inadequate for complete mineralization of azo dyes due to their chemical stability and resistance to biodegradation. These conventional approaches frequently result in the transfer of pollutants from one phase

[1] Department of Chemistry, G. E. Society's N. B. Mehta Science College Bordi, Tal. Dahanu, Dist. Palghar-401701, India.
[2] Research Centre and Department of Chemistry, Mahatma Gandhi Vidyamandir's Loknete Vyankatrao Hiray Arts, Science and Commerce College, Panchavati, Nashik-03, India.

* Author to whom correspondence should be addressed: prachidbhatewal@gmail.com (Prachi K. Bhoi)

© Ariston Publications 2026. All rights reserved.

to another rather than achieving complete degradation. Adsorption, while effective for concentrating the dye, merely transfers it to a solid phase that requires further disposal, and coagulation generates substantial sludge volumes that pose secondary pollution problems [3]. Biological treatment is often slow and unreliable for azo dyes because the electron-withdrawing azo groups are resistant to aerobic attack, while anaerobic cleavage can produce aromatic amines that are themselves toxic and potentially carcinogenic [1]. Consequently, there is an urgent need for more effective and sustainable treatment technologies capable of mineralizing these recalcitrant compounds into harmless by-products.

Photocatalytic degradation has emerged as a promising advanced oxidation process for the mineralization of recalcitrant organic pollutants, including azo dyes. This technology leverages semiconductor materials that, upon light irradiation, generate reactive oxygen species capable of breaking down complex organic molecules into harmless by-products such as CO_2, H_2O, and mineral acids. The photocatalysis process is considered green, simple, and economical compared to traditional treatment methods, offering advantages such as operation at ambient temperature and pressure, minimal secondary pollution, and the potential for solar energy utilization. The fundamental appeal of photocatalysis lies in its capacity for complete destruction rather than mere phase transfer, addressing the core limitation of adsorption and coagulation-based approaches.

The field of photocatalytic degradation of Congo red has expanded considerably over the past decade, with a growing body of literature examining diverse catalyst systems ranging from conventional metal oxides to complex ferrites, nanocomposites, and heterostructures. Titanium dioxide and zinc oxide remain the most extensively studied materials due to their stability and oxidizing power, though their wide bandgaps limit practical solar utilization [4]. Ferrite-based photocatalysts have attracted particular interest because their narrow bandgaps enable visible-light activation while their magnetic properties facilitate catalyst recovery and reuse [5]. Cerium substitution in spinel ferrites has further enhanced performance by introducing additional energy levels and promoting charge separation. Heterostructure designs, including combinations with graphene oxide, carbon nitride, and bismuth oxychloride, have demonstrated that rational interface engineering can suppress charge carrier recombination and extend light absorption [6]. Despite this progress, several critical gaps remain in the literature. Most studies focus on individual catalyst systems under optimized laboratory conditions, making direct comparisons across material classes difficult due to variations in light sources, reactor geometries, and degradation metrics. Furthermore, the mechanistic understanding of Congo red mineralization pathways, particularly the role of different reactive oxygen species and the nature of intermediate products, remains incomplete for many of the newer catalyst systems. Comprehensive toxicity assessments of treated effluents are rarely reported, leaving uncertainty about whether partial degradation products may pose risks comparable to the parent dye.

This review addresses these gaps by providing a systematic and critical evaluation of photocatalytic materials for Congo red degradation, with particular attention to structure-activity relationships, operational parameters that govern performance, and the mechanistic basis of dye mineralization. The novelty of this work lies in its integrated treatment of material classes that are typically reviewed in isolation, enabling cross-comparison of ferrites, metal oxides, and heterostructures on a common performance framework. Rather than merely cataloging reported efficiencies, this review examines the underlying factors that determine why certain materials outperform others and identifies the specific material design strategies that consistently yield high activity under visible light. By synthesizing mechanistic evidence from multiple catalyst systems, the review also clarifies the relative contributions of hydroxyl radicals, superoxide anions, and direct hole oxidation in Congo red degradation, providing a foundation for the rational design of more efficient photo-catalysts.

In this review, we report a comprehensive analysis of recent advances in photocatalytic degradation of Congo red dye, examining various photocatalyst materials, synthesis methodologies, degradation mechanisms, and operational parameters. The objective is to provide insights into the current state of knowledge, identify the most promising photocatalyst systems based on both performance and practical considerations, and outline future research directions for applications in industrial wastewater treatment.

2. CONGO RED DYE: PROPERTIES AND ENVIRONMENTAL IMPACT

Congo Red is an anionic azo dye derived from benzidine. It has the molecular formula $C_{32}H_{22}N_6Na_2O_6S_2$ and a molecular weight of 696.66 g.mol^{-1} [41]. The molecule consists of two naphthalene rings attached to each other via an azo dye group (two N=N functional groups). There are two azo groups attached to a biphynol core and two sulfonate functional groups (-SO_3Na) which make the molecule hydrophilic and anionic in aqueous conditions [42]. The molecule has a large conjugated system making it a highly coloured red dye. Due to this it is very stable towards chemical and biological breakdown. Figure 1 shows the structure of Congo Red.

The azo bonds are very important for the environmental impact of Congo Red. Under reducing conditions the azo bonds break down producing benzidine and other aromatic amines that are known to be carcinogenic to humans [43]. Therefore the toxicity of Congo Red cannot be solely determined based on the structure of the intact molecule. Congo Red is often found to be non-mutagenic in Ames testing. However it can become mutagenic if an external metabolic activating system is used [44]. This means that they are only mutagenic when converted into their active form by gut microbes or liver enzymes. This causes problems within the environment as there will be microbes in the sediment and water treatment systems that can reduce the azo groups to produce the toxic intermediates [45].

 © Ariston Publications 2026. All rights reserved.

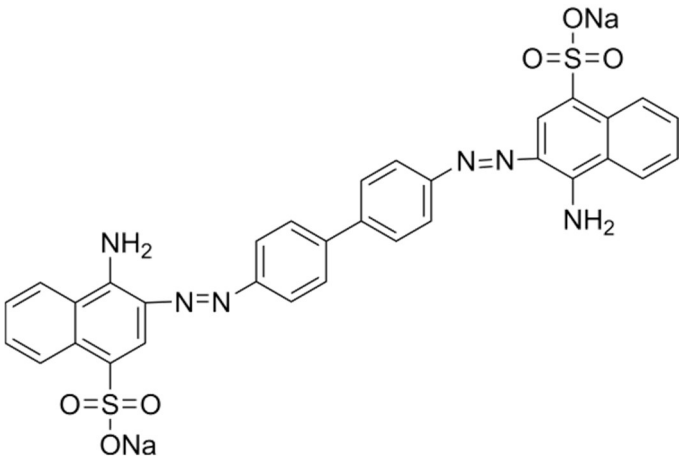


Fig. 1. Structure of Congo Red dye.

Congo Red can cause toxicity within different trophic levels. Microalgae are particularly affected by the dye. When exposed to concentrations between 5-25 mg L^{-1}, Chlorella vulgaris shows reduced growth rates, photosynthetic activity and respiration activity. Analysis of chlorophyll fluorescence showed that the donor side of Photosystem II had been damaged [46]. A comparative study was carried out using Pseudokirchneriella subcapitata, cladocerans and zebrafish embryos and the results showed that the microalgae were the most sensitive species to Congo Red. (IC_{50}= 3.11 mg L^{-1}). Zebrafish embryos displayed yolk sac oedema, skeletal deformities and difficulty hatching. [47] This shows that Congo Red can cause disruption to physiological functions within aquatic organisms.

Due to Congo Red absorbing strongly within the visible region, there will be less light penetration within aquatic environments. This will affect the macrophytes and phytoplankton as they will not receive enough light for photosynthesis. The dye can also directly inhibit photosynthetic electron transport, causing oxygen depletion and disrupting aquatic ecosystems [48]. Studies have shown that Congo Red can cause phytotoxicity within aquatic plants [49]. Studies have shown that the dye can interfere with the physiological functions of aquatic organisms directly and indirectly due to limiting light penetration. The dye and its breakdown products can also cause genotoxicity and carcinogenicity within mammals. This can cause issues if humans are exposed to contaminated drinking water. The dye can also bioaccumulate within edible aquatic organisms.

Due to Congo Red being so persistent, toxic and disruptive within the environment, it is considered a priority pollutant. Adsorption techniques will simply convert the dye into a solid state and biological methods can actually cause increased toxicity due to the azo bonds not being fully reduced [50]. Photocatalytic degradation methods can completely mineralise the dye. To design an effective photocatalyst it is important to understand the structure of the dye and how it behaves within the environment. This way the photocatalyst can specifically target the bonds within the molecule (azo bonds and aromatic rings) that cause the dye to be so stable and toxic.

3. PRINCIPLES OF PHOTOCATALYSIS

Photocatalysis is fundamentally a light-driven surface phenomenon occurring on semiconductor materials, wherein the absorption of photons with energy equal to or exceeding the bandgap energy (E_g) initiates a cascade of electronic and chemical events. When a semiconductor photocatalyst is irradiated, electrons (e^-) are excited from the valence band (VB) to the conduction band (CB), generating electron–hole pairs that subsequently migrate to the catalyst surface and participate in redox reactions with adsorbed species [51]. This charge separation event is the primary photophysical step governing the entire process, and its efficiency determines the overall quantum yield of the photocatalytic reaction. Figure 2 presents a schematic representation of the fundamental photocatalytic mechanism, illustrating the bandgap excitation, charge carrier migration, and generation of reactive oxygen species.

The mechanistic sequence of an ideal heterogeneous photocatalytic process can be expressed through the following set of reactions (Eqs. 1–12) [52-55]:

$$\text{Semiconductor} + h\upsilon \rightarrow \text{Semiconductor}\ (h^+\ VB + e^-\ CB) \quad (1)$$

$$h^+\ VB + e^-\ CB \rightarrow \text{heat} \quad (2)$$

$$OH^- + h^+\ VB \rightarrow \bullet OH \quad (3)$$

$$H_2O + h^+\ VB \rightarrow \bullet OH + H^+ \quad (4)$$

$$\bullet OH + \bullet OH \rightarrow H_2O_2 \quad (5)$$

$$e^- + H^+ + O_2 \rightarrow \bullet HO_2 \quad (6)$$

$$\bullet HO_2 + \bullet HO_2 \rightarrow O_2 + H_2O_2 \quad (7)$$

$$O_2 + e^- \rightarrow \bullet O_2^- \quad (8)$$

$$\bullet O_2^- + H^+ + \bullet HO_2 \rightarrow O_2 + H_2O_2 \quad (9)$$

$$H_2O_2 + e^- \rightarrow \bullet OH + OH^- \quad (10)$$

$$H_2O_2 + \bullet OH \rightarrow H_2O + \bullet HO_2 \quad (11)$$

$$\bullet OH + \text{organic substances} \rightarrow \text{intermediate} \rightarrow \text{product} \quad (12)$$

Equation (1) represents the primary excitation event, in which photon absorption promotes an electron from the VB to the CB, leaving a hole behind. Equation (2) accounts for the competitive recombination of these charge carriers, dissipating the absorbed energy as heat, a loss pathway that directly limits quantum efficiency. Equations (3)–(5) describe the oxidative route: photogenerated holes react with surface hydroxyl ions or water to produce hydroxyl radicals

© Ariston Publications 2026. All rights reserved.

(•OH), which can further combine to form hydrogen peroxide. Equations (6)–(11) describe the reductive route: conduction-band electrons reduce dissolved oxygen to superoxide ($•O_2^-$) and hydroperoxyl ($•HO_2$) radicals, with subsequent transformations yielding H_2O_2 and additional •OH. Equation (12) represents the ultimate degradation step, in which •OH attacks the organic pollutant, converting it through intermediates to final products.

The photogenerated holes (h^+) residing in the valence band possess strong oxidizing capability and can either directly oxidize organic pollutants through interfacial electron transfer or react with water molecules and hydroxyl ions to produce hydroxyl radicals (•OH) [52]. Simultaneously, electrons in the conduction band reduce molecular oxygen adsorbed on the catalyst surface to form superoxide radicals ($•O_2^-$). These reactive oxygen species are highly reactive and non-selective, capable of attacking a broad range of organic molecules and driving their mineralization through successive oxidation steps [53]. The relative dominance of each reactive species depends on the band edge positions of the semiconductor, the dissolved oxygen concentration, and the solution pH, which collectively determine whether hydroxyl radical oxidation, superoxide radical attack, or direct hole transfer constitutes the principal degradation pathway for a given pollutant–catalyst system.

In aqueous media, the overall photocatalytic process can be described as a sequence of five interconnected stages [30]: (i) transfer of pollutants from the liquid phase to the catalyst surface; (ii) adsorption of pollutants onto the activated catalyst surface; (iii) photogeneration of reactive oxygen species (ROS), including •OH, followed by pollutant degradation; (iv) desorption of intermediates from the catalyst surface; and (v) transfer of intermediates back into the liquid phase. Because surface reactions play a decisive role in the mechanism, the adsorption of reactants on the semiconductor surface is of great importance [31]. The mode of adsorption, chemisorption versus physiosorption, can determine whether degradation proceeds via direct hole oxidation or indirect ROS-mediated pathways. For instance, formic acid chemisorbs strongly on titania in water and is oxidized directly by trapping photogenerated holes, whereas benzene is physisorbed and undergoes indirect photo-oxidation; phenol exhibits both modes depending on the solvent [31]. In addition to the reactants, the binding strength of products and intermediates to the catalyst surface is also critical, as strongly bound species can block active sites and hinder further oxidation [31]. Interactions between water and the photocatalyst surface must likewise be considered when determining the operative mechanism.

The efficiency of photocatalytic degradation is governed by several interconnected material and operational factors. Bandgap energy dictates the spectral range of light absorption, with an ideal photocatalyst absorbing visible light (approximately 1.8–3.0 eV) to maximize solar energy utilization [54]. Charge carrier separation and transport determine how many photogenerated electrons and holes reach the surface before recombining, and recombination losses (Eq. 2) remain one of the most significant limitations in practical photocatalyst design. Surface area and crystallinity influence the density of active sites available for adsorption and reaction, while surface defects can either serve as catalytic active centers or act as recombination traps depending on their nature and concentration [55].

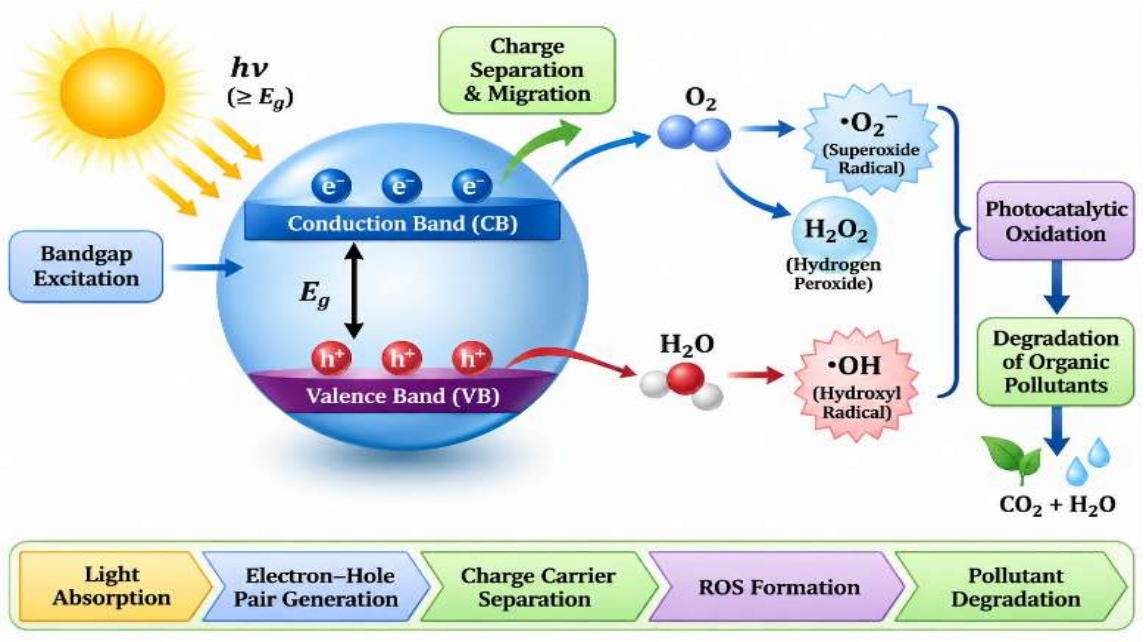


Fig. 2. Schematic representation of the fundamental photocatalytic mechanism on a semiconductor surface, illustrating light-induced bandgap excitation, electron–hole pair generation, charge-carrier separation and migration, reactive oxygen species (ROS) formation, and subsequent photocatalytic degradation of organic pollutants.

© Ariston Publications 2026. All rights reserved.

An effective photocatalyst must therefore strike a balance among these often-competing properties, achieving sufficient light absorption, efficient charge separation, and adequate surface reactivity without sacrificing chemical stability under operational conditions. Recent mechanistic investigations have clarified how reactive oxygen species mediate the degradation of azo dyes specifically. Scavenger studies on ZnO/g-C_3N_4 nanocomposites employed for Congo red degradation identified superoxide radicals as the dominant reactive species in that system, with hydroxyl radicals and holes playing secondary roles [56]. This finding underscores an important principle: the identity of the dominant reactive species is not universal but depends on the specific band structure of the photocatalyst. Materials with sufficiently negative conduction band potentials favor the one-electron reduction of oxygen to superoxide (Eq. 8), whereas catalysts with deeply positioned valence bands promote hydroxyl radical generation through water oxidation (Eqs. 3–4). Understanding these material-specific mechanistic distinctions is essential for rational catalyst design, as it enables researchers to select or engineer photocatalysts whose band edge positions align with the desired reactive pathway for a target pollutant.

The timescales of the elementary processes involved further illuminate the challenges inherent in photocatalyst optimization. Charge carrier generation occurs on the femtosecond timescale, while recombination typically transpires within nanoseconds to microseconds, often before carriers can reach the surface and participate in productive chemistry. Interfacial charge transfer to adsorbed species occurs on timescales ranging from picoseconds to milliseconds, and the subsequent chemical reactions proceed over milliseconds to seconds [57]. This hierarchy of timescales means that even modest improvements in charge separation efficiency can translate into substantial gains in overall photocatalytic performance, which explains the intense research focus on heterojunction formation, doping, and defect engineering as strategies to suppress recombination and extend carrier lifetimes.

4. MECHANISMS OF AZO DYE DEGRADATION

The photocatalytic degradation of azo dyes such as Congo red is not a single elementary reaction but a network of parallel and sequential pathways involving both direct and indirect oxidation mechanisms [12, 52]. The direct route entails interfacial electron transfer from the adsorbed dye molecule to photogenerated valence-band holes, whereas the indirect route proceeds through reactive oxygen species (ROS) generated at the catalyst surface. In most illuminated semiconductor systems, the indirect pathway dominates, and the primary mechanism involves the generation of ROS that attack the azo bonds and aromatic rings of the dye [53].

Among the ROS, hydroxyl radicals (•OH) are particularly effective owing to their high oxidation potential (2.8 V vs. NHE) and non-selective reactivity, which allows them to attack a broad spectrum of organic functionalities without substrate specificity [52]. Superoxide radicals ($•O_2^-$) also contribute to degradation by attacking electron-rich sites in the dye molecule, particularly the azo linkage and the amino-substituted naphthalene rings, although their oxidation potential is lower than that of •OH [56]. The relative contribution of different reactive species is not universal but depends on the photocatalyst properties, pH conditions, and dissolved oxygen concentration, which together determine the band edge positions, the surface charge, and the availability of adsorbed oxygen [55].

The degradation typically follows a stepwise process. The first stage is the initial attack on the azo bonds (–N=N–), which leads to rapid decolorization as the chromophoric conjugation is disrupted; this step is frequently the fastest and is readily monitored by the decline in absorbance at the dye's characteristic visible maximum [12]. The second stage involves breakdown of the aromatic rings through hydroxylation and ring-opening reactions, producing smaller organic intermediates such as substituted phenols, naphthols, and short-chain carboxylic acids. The third stage comprises further oxidation of these intermediates, and the fourth stage is complete mineralization to CO_2, H_2O, and inorganic ions such as sulfate and nitrate [11]. It is important to recognize that decolorization is not equivalent to mineralization; a solution may appear colorless while still containing aromatic intermediates of residual toxicity, which is why total organic carbon removal and toxicity assessment are essential complements to colorimetric measurements [12].

The mechanistic sequence is commonly represented through the heterogeneous photocatalytic reactions summarized in Eqs. (1)–(12), in which •OH is generated both by hole oxidation of water and hydroxide ions (Eqs. 3–4) and by reduction of H_2O_2 (Eq. 10), while $•O_2^-$ forms through one-electron oxygen reduction (Eq. 8). Equation (12) captures the terminal step in which •OH attacks the organic substrate, converting it through intermediates to final products. Scavenger studies provide experimental support for these assignments: in ZnO/g-C_3N_4 nanocomposites applied to Congo red, superoxide radicals were identified as the dominant species, with hydroxyl radicals and holes playing secondary roles [56], whereas in ferrite-based systems the emphasis shifts toward •OH-mediated oxidation [10, 11]. This material dependence underscores that rational catalyst design must align band edge positions with the desired reactive pathway rather than assume a universal mechanism.

5. PHOTOCATALYST MATERIALS AND SYNTHESIS METHODS

The design and synthesis of photocatalysts for Congo red degradation have evolved considerably over the past decade, moving from conventional wide-bandgap semiconductors toward engineered materials with tailored electronic structures, enhanced visible-light responsiveness, and improved recoverability. The literature reveals a clear trajectory: early work centered on TiO_2 and ZnO as benchmark systems, while contemporary research

© Ariston Publications 2026. All rights reserved.

increasingly favors ferrite-based magnetic materials and heterostructured nanocomposites that address the fundamental limitations of charge recombination and catalyst recovery. What follows examines the principal material families that have emerged from this research effort, organized according to their compositional logic and the synthesis strategies that govern their performance.

5.1. Metal oxide-based photocatalysts

Metal oxides constitute the most extensively investigated class of materials for Congo red photodegradation, largely because of their chemical robustness, low toxicity, and well-understood surface chemistry. Titanium dioxide remains the reference material against which new candidates are judged, yet its anatase bandgap of 3.2 eV confines photoactivation to the ultraviolet region, which represents only a small fraction of the solar spectrum. Ullah et al. addressed this constraint through tungsten doping of TiO_2 synthesized by a sol–gel route, demonstrating that 6 mol% W incorporation extends the excitation wavelength into the visible range while simultaneously suppressing electron–hole recombination through the formation of intermediate energy levels within the bandgap [7]. The doped catalyst outperformed commercial Degussa P25 under both UV and visible illumination, and a thin-film configuration enabled straightforward catalyst recovery and reuse [2]. This work illustrates a general principle in metal oxide photocatalysis: substitutional doping with transition metals whose ionic radii closely match the host cation can modulate band structure without destabilizing the lattice.

Zinc oxide has attracted comparable attention, though its practical deployment has been complicated by photocorrosion under prolonged irradiation. Khairol et al. adopted an unusual electrosynthesis approach to deposit ZnO nanoparticles directly onto eggshell substrates, producing a bio-templated catalyst that achieved 91.6% Congo red removal at pH 3 with a catalyst loading of 1 g L^{-1} [8]. The porous eggshell support contributed both to material economy and to enhanced surface area, while the acidic optimum reflected the electrostatic attraction between the protonated ZnO surface and the anionic sulfonate groups of Congo red [8]. Sangon et al. extended the biomass-derived concept further by developing rice straw-derived mesoporous carbon–ZnO nanocomposites through a single-step zinc chloride activation process [9]. The resulting material exhibited a specific surface area of 942.7 m^2 g^{-1} with 99% mesoporosity, and the retention of ZnO within the carbon matrix produced a dual-function adsorbent–photocatalyst capable of removing both cationic and anionic dyes [9]. The synergy between adsorption and photocatalysis in this system is instructive: the carbon framework concentrates dye molecules near the ZnO active sites, partially decoupling degradation kinetics from bulk solution concentration.

Yttrium oxide represents a contrasting case. Michel et al. prepared nanostructured Y_2O_3 by coprecipitation and evaluated its activity against both Congo red and malachite green [10]. Despite the wide bandgap of Y_2O_3 (4.86–5.68 eV), the material achieved approximately 24% photocatalytic degradation of Congo red after 60 minutes of UV exposure (Figure 3), supplemented by a 22% contribution from dissociative adsorption [10]. The striking disparity between Congo red (24%) and malachite green (94%) degradation efficiencies underscores how profoundly dye molecular structure and charge characteristics influence degradation outcomes, a point that is sometimes overlooked in comparative material assessments [10]. Nickel oxide nanostructures prepared by hydrothermal synthesis have demonstrated markedly higher performance, with reported degradation approaching 98% [11]. The hydrothermal route yields well-crystallized particles with controlled morphology and high surface area, and the favorable band alignment of NiO supports efficient generation of reactive oxygen species under illumination [11].

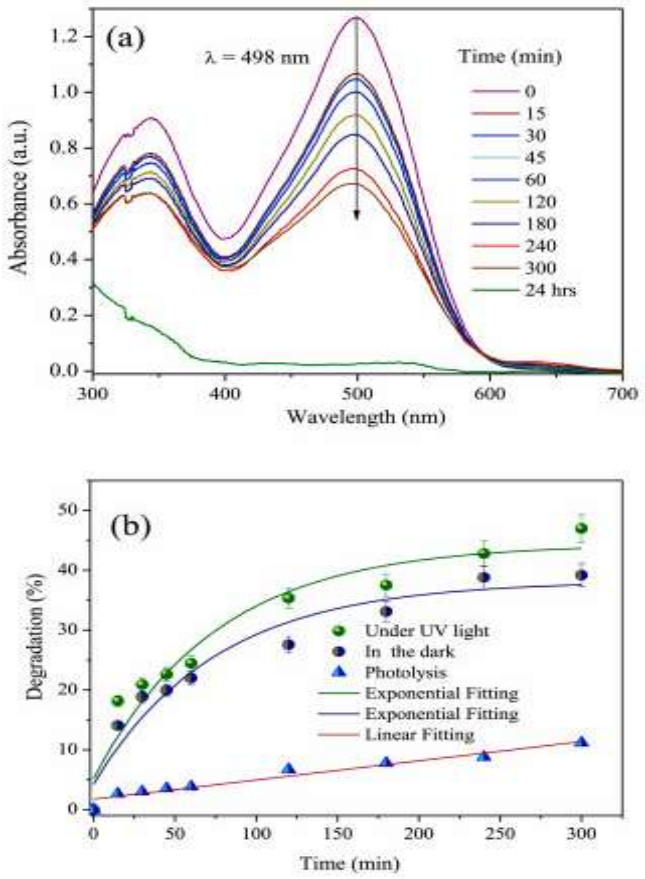


Fig. 3. (a) UV–vis absorbance spectra showing the degradation of Congo red (CR) by Y_2O_3; (b) Graphs of degradation percentages with time. Reprinted from ref. [10], Michel, C.R. and Martínez-Preciado, A.H., 2023. Adsorption and photocatalytic degradation of Congo red and malachite green by nanostructured Y_2O_3 synthesized by the coprecipitation method. *Open Ceramics*, *13*, p.100336. https://doi.org/10.1016/j.oceram.2023.100336. Copyright under the Creative Commons CC-BY-NC-ND license © Elsevier B.V.

© Ariston Publications 2026. All rights reserved.

5.2. Ferrite-based photocatalysts

The ferrite family has emerged as arguably the most promising class of materials for practical Congo red treatment, primarily because spinel ferrites combine visible-light activity with magnetic recoverability, a combination that addresses both the energetic and the operational limitations of conventional oxide photocatalysts. Vijayaraghavan et al. synthesized alkaline earth ferrites AFe_2O_4 (A = Ba, Ca, Sr) by sol–gel method and reported bandgap energies in the narrow range of 2.14–2.19 eV, well suited to visible-light absorption [12]. Under xenon lamp irradiation, $BaFe_2O_4$ achieved 92% Congo red degradation after 75 minutes, while $CaFe_2O_4$ exhibited the fastest kinetics, reaching 70% removal within just 15 minutes. Notably, $SrFe_2O_4$ displayed the highest adsorption capacity (44% after 75 minutes in the absence of light), indicating that surface adsorption contributes meaningfully to overall dye removal in these systems [12]. The orthorhombic crystal structures of these ferrites, with varying space groups depending on the alkaline earth cation, illustrate how A-site substitution can tune both electronic and surface properties without altering the fundamental spinel architecture.

Rare-earth substitution has proven particularly effective in enhancing ferrite performance. Dinesh et al. prepared cerium-substituted Mn–Zn ferrites ($Mn_{0.5}Zn_{0.5}Ce_xFe_{2-x}O_4$) via sol–gel combustion synthesis, with the composition $Mn_{0.5}Zn_{0.5}Ce_{0.3}Fe_{1.7}O_4$ achieving 97.25% Congo red degradation within 120 minutes under visible light [13]. The cerium incorporation serves multiple functions: it introduces 4f energy levels within the bandgap that facilitate visible-light absorption through f–d transitions, and the accessible Ce^{3+}/Ce^{4+} redox couple promotes electron transfer while suppressing charge carrier recombination [13]. The ferromagnetic behavior of these nanoparticles permits magnetic separation and reuse, a practical advantage that is difficult to overstate for wastewater treatment applications. Ramadoss et al. investigated mesoporous manganese ferrite nanoparticles for Congo red mineralization and reported a point of zero charge of 6.7, which creates favorable electrostatic conditions for anionic dye adsorption at circumneutral pH [14]. The mesoporous structure provides abundant active sites, and the ferromagnetic properties again enable magnetic recovery [14]. Riyanti et al. examined $MgFe_2O_4$ as a magnetic catalyst under visible light, focusing on the influence of solution pH and initial dye concentration on degradation efficiency, thereby contributing valuable operational data for scale-up considerations [15].

5.3. Nanocomposites and heterostructures

The formation of heterojunctions between complementary semiconductor phases represents a deliberate strategy to overcome the intrinsic limitations of single-component materials, particularly the rapid recombination of photogenerated charge carriers that limits quantum efficiency. Chate et al. developed titania nanostructure bunches decorated on graphene oxide (TiO_2–GO–N), achieving approximately 92% Congo red degradation efficiency [6]. The graphene oxide component contributes through multiple mechanisms: π–π conjugation extends light absorption, the heterojunction interface promotes charge separation, the high surface area enhances dye adsorption, and the graphene network provides efficient electron transport pathways [6]. The result is a synergistic enhancement that exceeds what either component could achieve independently.

Chowdhury et al. reported a CS–BiOCl/ZnO ternary nanocomposite fabricated by a modified hydrothermal route that achieved 93% Congo red degradation under UV light within 40 minutes [20]. The type-II band alignment between BiOCl and ZnO facilitates spatial separation of electrons and holes, reducing recombination losses, while the chitosan matrix serves as a biocompatible, dye-adsorbing scaffold that also imparts structural integrity to the composite [20]. Yu et al. investigated carbon nitride-based nanocomposites incorporating zinc terpyridyl coordination polymers, exploiting the visible-light activity and chemical stability of g-C_3N_4 while introducing additional active sites and modified electronic structure through the coordination polymer component [31].

Basurrah et al. developed a magnetically recoverable $NiFe_2O_4$–MWCNT–CA nanocomposite for the UV-driven photodegradation of organic pollutants, including Congo red [58]. Biogenic $NiFe_2O_4$ nanoparticles were synthesized using *Costus speciosus* extract, yielding a crystallite size of 32.5 nm that increased to 83.6 nm upon incorporation into the multi-walled carbon nanotube (MWCNT)–cellulose acetate (CA) matrix. X-ray diffraction confirmed preservation of the cubic spinel structure, while vibrating sample magnetometry showed retained ferrimagnetic behavior with a saturation magnetization of 9.64 emu/g, enabling rapid magnetic separation. Although BET analysis revealed a reduction in surface area from 112.46 to 30.99 m^2/g due to pore blockage by the polymer and carbon components, the conductive MWCNT network significantly enhanced charge separation and interfacial electron transport. The composite displayed a widened optical bandgap of 5.3 eV, necessitating UV excitation. Under UV irradiation, the composite achieved 97 % degradation of methylene blue and 91% degradation of Congo red at 20 mg/L, with corresponding rate constants of 0.119 and 0.076 min^{-1} (Figure 4). Scavenger experiments confirmed hydroxyl radicals (•OH) as the dominant reactive species, followed by photogenerated holes (h^+). Zeta potential measurements showed a shift from −44.97 mV for pristine $NiFe_2O_4$ to −14.42 mV for the composite, indicating partial surface coverage by CA and MWCNTs. These heterostructure approaches share a common design philosophy: rather than seeking a single material with optimal properties, they combine materials whose individual strengths compensate for each other's weaknesses.

5.4. Novel and emerging materials

Beyond the established material families, several

© Ariston Publications 2026. All rights reserved.

unconventional candidates have demonstrated notable performance. Tungsten disulfide nanoparticles achieved greater than 95% degradation of a ternary dye mixture containing Congo red within 40 minutes under visible light, with an optimum catalyst loading of 1.2 g L^{-1} for an initial dye concentration of 7 mg L^{-1} [17].

The layered structure of WS_2 provides abundant edge sites that serve as catalytically active centers, and the material exhibited remarkable stability across a pH range of 2–8 without structural alteration after photodegradation, enabling effective recycling [17]. Tin ferrite ($SnFe_2O_4$) nanocrystals synthesized by hydrothermal method displayed shape-dependent photocatalytic behavior, with nanocubes achieving 92% Congo red degradation and superior photoelectrochemical performance compared to nanodisks, highlighting the sensitivity of photocatalytic activity to exposed crystal facets and surface energy [16]. Delta-phase manganese dioxide (δ-MnO_2) nanostructures achieved moderate Congo red degradation exceeding 50%, with performance influenced by pH, dye concentration, and catalyst dosage [18]. While less efficient than the ferrite systems, δ-MnO_2 offers advantages of low cost, environmental compatibility, and synthetic accessibility that may be relevant for contexts where high-end performance is not the primary constraint. Finally, Princy et al. demonstrated a green synthesis route for spherical silver nanoparticles using Hibiscus cannabinus seed extract, in which plant-derived phytochemicals serve as reducing and capping agents, eliminating the need for toxic reagents [19]. This biogenic approach represents a broader movement toward sustainable nanomaterial synthesis, though the photocatalytic efficiency of such systems for Congo red degradation remains modest compared to engineered ferrites and heterostructures.

6. PHOTOCATALYTIC DEGRADATION PERFORMANCE: PROCESS PARAMETERS AND MECHANISTIC CONSIDERATIONS

The photocatalytic degradation of Congo red is governed by a complex interplay of material-intrinsic properties and extrinsic operational variables, and the literature reveals that reported efficiencies ranging from approximately 24% to 98% cannot be meaningfully compared without careful attention to the conditions under which they were obtained. This section examines the performance landscape through the lenses of degradation efficiency and kinetics, operational parameter sensitivity, light source requirements, mechanistic pathways, and the practical advantages and limitations that determine whether a given photocatalytic system is viable for real-world application.

6.1. Degradation efficiency and kinetics

Among the materials surveyed in this review, nickel oxide nanostructures prepared by hydrothermal synthesis reported the highest single-material efficiency at 98% [6], followed closely by cerium-substituted Mn–Zn ferrite at 97.25% [8] and tungsten disulfide nanoparticles exceeding 95% [14]. These high-performing systems share several characteristics: bandgap energies suitably positioned for the excitation source employed, high surface areas that maximize dye–catalyst contact, and electronic structures that suppress charge carrier recombination to a degree sufficient for reactive oxygen species to accumulate at catalytically relevant concentrations.

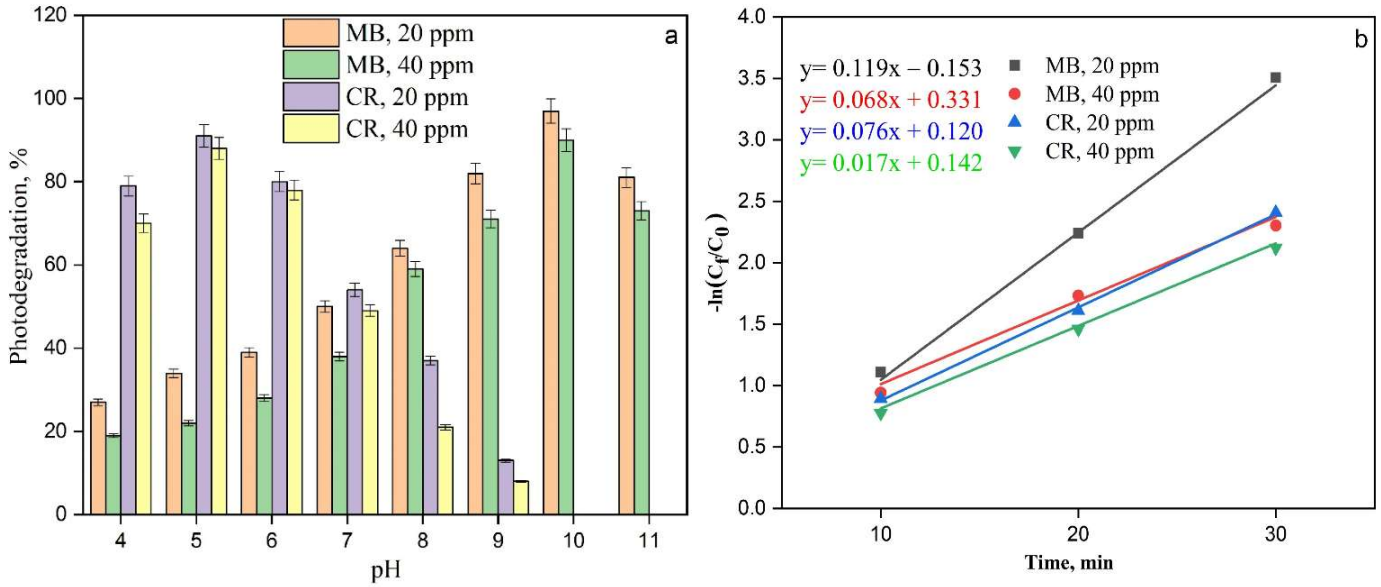


Fig. 4. Photodegradation performance of MB and CR: (a) pH effect, and (b) pseudo-first-order kinetic analysis at 20 and 40 ppm. Reprinted from ref. [58], Assem, B., Althobaiti, I.O. and Almulaiky, Y.Q., 2026. Synergistic and Magnetically Recoverable $NiFe_2O_4$–MWCNT–CA Nanocomposites for Efficient UV-Driven Photodegradation of Organic Pollutants. *Catalysts*, *16*(3), p.262. https://doi.org/10.3390/catal16030262. Copyright © Creative Commons Attribution (CC BY) license, MDPI.

© Ariston Publications 2026. All rights reserved.

Ferrite-based materials and heterostructures occupy a consistently strong position in the performance hierarchy, with $BaFe_2O_4$ and $SnFe_2O_4$ each achieving 92% degradation [7, 15], the CS–BiOCl/ZnO ternary composite reaching 93% under UV illumination [12], and the TiO_2–graphene oxide heterostructure attaining approximately 92% [11]. The convergence of these values around the 92–93% range across chemically distinct systems suggests that while material design can reliably deliver high removal percentages, pushing beyond this threshold toward near-complete mineralization requires more than compositional optimization alone.

Galloni et al. comparatively investigated pristine Co_3O_4 and a $CuCo_2O_4$-based mixed oxide for the removal of two chemically distinct anionic dyes, methyl orange (MO) and Congo red (CR), under solar irradiation [59]. Rather than focusing solely on maximizing removal efficiency, the study examined how material–pollutant interactions govern pollutant-dependent removal behavior. Under solar irradiation, Co_3O_4 achieved 94% MO removal within 180 min at acidic pH, whereas CR removal showed a stronger adsorption contribution (Figure 5). Conversely, the $CuCo_2O_4$-based oxide exhibited near-complete CR removal through adsorption but limited photocatalytic contribution toward MO. After regeneration, substantial recovery of both photocatalytic and adsorption performance was observed. These complementary behaviors were exploited in sequential treatment of a binary MO/CR mixture, combining CR removal by adsorption over the $CuCo_2O_4$-based material with photocatalytic removal of residual MO by Co_3O_4.

Kinetic behavior reveals a more nuanced picture than terminal efficiency values. $CaFe_2O_4$ demonstrated the fastest initial degradation rate among the surveyed materials, achieving 70% Congo red removal within 15 minutes [7], whereas the cerium-substituted Mn–Zn ferrite required 120 minutes to reach 97.25% [8]. This distinction matters for practical implementation: a material that removes 70% of the dye in 15 minutes may be preferable for a continuous-flow reactor with short hydraulic residence times, while a slower but more thorough system may suit batch treatment where contact time is not the limiting constraint. The kinetics reflect underlying differences in light absorption efficiency, charge carrier mobility, and the density and accessibility of surface active sites. At the lower end of the performance spectrum, Y_2O_3 nanostructures achieved only 24% photocatalytic degradation under UV exposure, supplemented by 22% adsorption [5], while δ-MnO_2 nanostructures reached approximately 50% [16]. These modest efficiencies trace to identifiable material limitations: the wide bandgap of Y_2O_3 restricts photoactivation to a narrow UV window, and both systems exhibit suboptimal charge separation characteristics. Their inclusion in the literature nonetheless serves a valuable function, illustrating that material selection must balance performance against cost, availability, and synthetic simplicity rather than pursuing efficiency as an isolated objective.

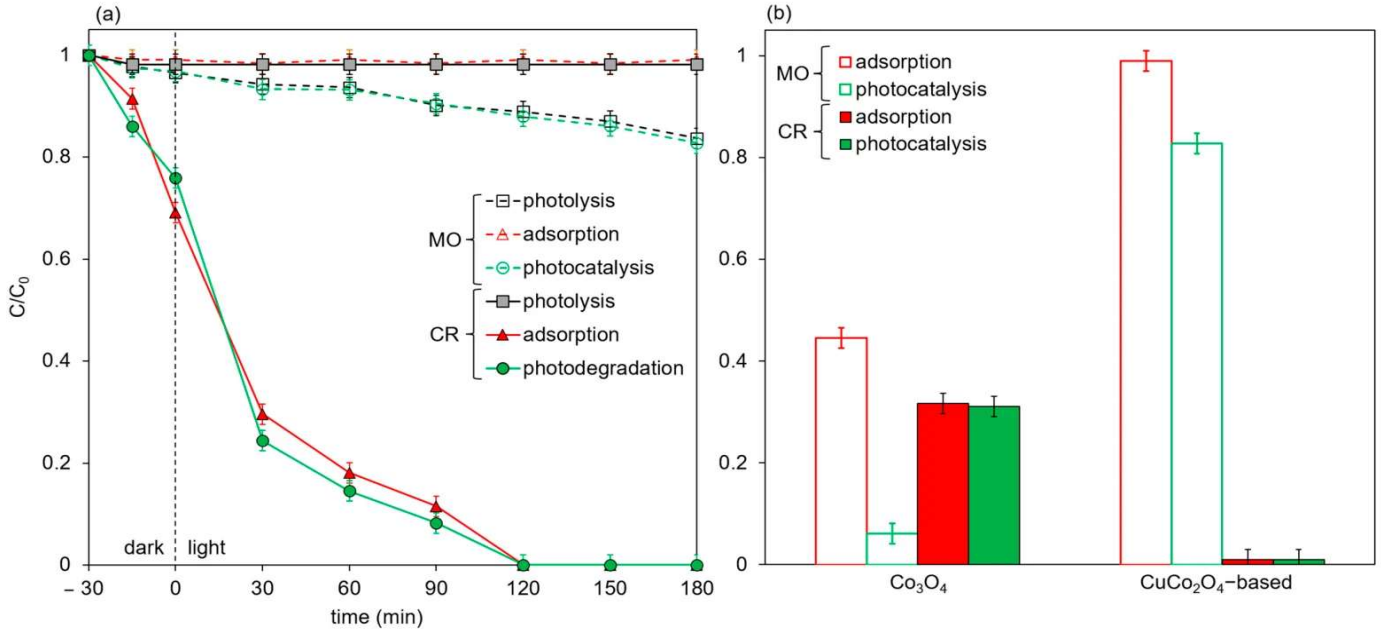


Fig. 5. (a) Methyl orange (MO) and Congo red (CR) abatement in UW by photolysis, adsorption and photocatalysis on the $CuCo_2O_4$-based sample. (b) Comparison of the adsorption and photocatalytic performances of the Co_3O_4 and $CuCo_2O_4$-based samples toward MO and CR. Reprinted from ref. [59], Galloni, M.G., Fabbrizio, V., Nasirova, G., Falletta, E., Giordana, A., Cerrato, G. and Bianchi, C.L., 2026. From Selective Adsorption to Photocatalytic Removal: Complementary Cobalt Oxides for Pollutant-Oriented Treatment of Dye Mixtures. *Catalysts*, *16*(10), p.885. https://doi.org/10.3390/catal16100885, Copyright © Creative Commons Attribution (CC BY) license, MDPI.

© Ariston Publications 2026. All rights reserved.

6.2. Influence of operational parameters

Solution pH exerts a pronounced influence on degradation efficiency by simultaneously modulating catalyst surface charge and dye speciation. The point of zero charge (pH PZC) defines the pH at which the catalyst surface transitions from net positive to net negative, and for anionic dyes such as Congo red, conditions below the pH PZC favor electrostatic attraction between the protonated catalyst surface and the sulfonate groups of the dye. Ramadoss et al. reported a pH PZC of 6.7 for mesoporous manganese ferrite nanoparticles, implying favorable adsorption conditions at circumneutral and mildly acidic pH [9]. Not all materials exhibit this sensitivity, however. WS_2 nanoparticles maintained consistent degradation efficiency across a pH range of 2–8 [14], a robustness that is advantageous for treating wastewaters whose pH may fluctuate or lie outside the range amenable to pH adjustment. Catalyst dosage represents a second critical variable, with an optimum existing between the extremes of insufficient active sites and excessive light attenuation. Patel et al. identified 1.2 g L^{-1} as optimal for WS_2 at an initial dye concentration of 7 mg L^{-1} [14], and the general pattern observed across studies is consistent: degradation efficiency rises with catalyst loading up to a point beyond which increased turbidity reduces photon penetration and the photoactivated volume of the suspension declines [citation:10 from search results]. Initial dye concentration introduces a further constraint, as higher concentrations demand proportionally more reactive oxygen species for mineralization and may saturate catalyst surfaces through competitive adsorption. The studies reviewed employed concentrations ranging from 7 mg L^{-1} [14] to values examined comparatively by Michel et al. [5], and the consistent finding is that lower initial concentrations yield higher percentage removal within a given irradiation period, though the absolute mass of dye degraded may be greater at higher concentrations.

6.3. Light source requirements

The distinction between UV-activated and visible-light-active photocatalysts carries substantial implications for energy consumption and operational cost. Visible-light photocatalysts can exploit solar radiation, which contains approximately 45% visible light compared with only 5% UV, thereby reducing or eliminating the need for artificial illumination. Ferrite-based materials exemplify this advantage: their bandgap energies of 2.14–2.19 eV position them squarely within the visible spectrum [7], and the cerium-substituted Mn–Zn ferrite achieved its 97.25% efficiency under visible light [8], while alkaline earth ferrites performed well under both xenon lamp and natural sunlight [7]. WS_2 nanoparticles likewise demonstrated strong visible-light activity exceeding 95% degradation [14]. In contrast, several high-performing systems remain UV-dependent. Y_2O_3 was evaluated under 365 nm UV illumination [5], and the CS–BiOCl/ZnO nanocomposite achieved its 93% efficiency under UV light [12]. Tungsten-doped TiO_2 represents a deliberate strategy to bridge this divide, with doping extending absorption into the visible range while preserving activity under UV as well [2]. The practical significance is straightforward: a photocatalyst that performs optimally under UV requires electricity for lamp operation, whereas a visible-light-active material may operate under ambient solar illumination, fundamentally altering the economics of treatment at scale.

6.4. Mechanistic insights and reactive species

The degradation of Congo red proceeds through the generation and action of reactive oxygen species, with hydroxyl radicals (•OH) and superoxide anions ($\bullet O_2^-$) identified as the principal agents of mineralization. Direct spectroscopic evidence for ROS generation was provided by Michel et al., whose XPS analysis of Y_2O_3 surfaces revealed increased hydroxyl group density following photocatalytic testing [5], consistent with hole-mediated oxidation of water or hydroxide ions. The degradation sequence unfolds in stages: initial attack on the azo bonds (–N=N–) disrupts the chromophoric conjugation and produces rapid decolorization, followed by hydroxylation and ring-opening of the aromatic systems, generation of smaller organic intermediates, and ultimately mineralization to CO_2, H_2O, and inorganic ions including sulfate and nitrate. Recent LC-MS analysis of Congo red degradation by a CuO–ZnO/HAP composite has provided finer mechanistic resolution, showing that superoxide radicals primarily drive initial azo bond cleavage whereas hydroxyl radicals are more prominent in desulfonation and ring-opening steps [citation:5 from search results]. This division of labor among reactive species reinforces the principle that the dominant pathway is material-specific: photocatalysts with deeply positioned valence bands favor •OH generation, while those with sufficiently negative conduction band potentials promote $\bullet O_2^-$ formation through one-electron oxygen reduction. The synergistic participation of multiple ROS typically yields more complete mineralization than any single species could achieve in isolation.

Adsorption frequently operates alongside photocatalysis as a complementary removal mechanism, and in some systems its contribution is substantial. Michel et al. reported 22% dissociative adsorption in addition to 24% photocatalytic degradation for Y_2O_3 [5], while Vijayaraghavan et al. observed 44% dye adsorption by $SrFe_2O_4$ in the absence of illumination [7]. This synergy is particularly pronounced in nanocomposites incorporating high-surface-area components such as graphene oxide or mesoporous carbon, where adsorption concentrates dye molecules near photocatalytic active sites and partially decouples reaction kinetics from bulk solution concentration. The distinction between adsorption and degradation is not merely academic: adsorption transfers the pollutant to a solid phase that must then be regenerated or disposed of, whereas degradation mineralizes it. A material that removes dye

 © Ariston Publications 2026. All rights reserved.

primarily by adsorption may appear efficient in colorimetric assays while offering no true destruction of the pollutant.

7. ADVANTAGES, LIMITATIONS, AND PERSISTENT CHALLENGES

Photocatalytic degradation offers compelling advantages for Congo red treatment: operation at ambient temperature and pressure, no requirement for chemical additives, and the capacity for complete mineralization rather than phase transfer. Magnetic ferrite photocatalysts add the practical benefit of facile recovery and reuse through magnetic separation, addressing a central concern in catalyst deployment [8, 9]. Yet the path from laboratory demonstration to industrial implementation is obstructed by several persistent limitations. Charge carrier recombination remains the most fundamental constraint on quantum efficiency, as photogenerated electrons and holes recombine on nanosecond to microsecond timescales that often precede their arrival at the surface. Many high-performance materials still require UV activation, and those that function under visible light often exhibit lower quantum yields than their UV-activated counterparts. Catalyst stability over extended operation is another concern: while WS_2 showed no structural alteration after photodegradation [14], other materials are susceptible to photocorrosion, metal ion leaching, or deactivation through intermediate adsorption. The scalability of synthesis and the cost of precursors present further barriers, though green synthesis routes using agricultural waste [4] or plant extracts [17] offer partial mitigation. Finally, the formation of toxic intermediates during incomplete degradation demands attention, and the demonstration by Ramadoss et al. of mineralization to non-toxic by-products [9] represents an important benchmark that few studies have matched with comprehensive toxicity assessment.

8. FUTURE DIRECTIONS AND RECOMMENDATIONS

Future research should focus on several key areas to advance photocatalytic technology toward practical wastewater treatment applications. The development of highly efficient visible-light-active photocatalysts remains a priority. Strategies such as bandgap engineering through doping, heterostructure formation, and plasmonic enhancement should be further explored to maximize solar energy utilization. The incorporation of rare earth elements, as demonstrated by the cerium-substituted ferrites [10], represents a promising approach that warrants further investigation with other rare earth dopants. Mechanistic studies using advanced characterization techniques are needed to elucidate the detailed degradation pathways and identify rate-limiting steps. In-situ spectroscopic techniques, such as electron paramagnetic resonance (EPR) for reactive species detection and time-resolved spectroscopy for charge carrier dynamics, can provide valuable insights for rational catalyst design. The development of multifunctional photocatalysts that combine high activity, magnetic recoverability, and long-term stability is essential for practical applications. Ferrite-based materials show promise in this regard, but further optimization of composition and morphology is needed to maximize performance [10, 11]. Scale-up studies and pilot-scale demonstrations are critically needed to bridge the gap between laboratory research and industrial implementation. These studies should address issues such as reactor design, light distribution, mass transfer limitations, and catalyst recovery in continuous-flow systems. Economic analyses comparing photocatalytic treatment with conventional methods will help identify the most cost-effective applications and operating conditions. The integration of photocatalysis with other treatment technologies, such as membrane filtration or biological treatment, may offer synergistic benefits and improved overall performance. Hybrid systems could leverage the strengths of each technology while mitigating individual limitations. Finally, the development of sustainable and cost-effective synthesis methods using abundant raw materials, agricultural waste, or biogenic approaches should be prioritized [8, 18]. This will reduce material costs and environmental impact while promoting circular economy principles in photocatalyst production.

9. CONCLUSION

This review of photocatalytic degradation of Congo red dye documents substantial progress in the development of efficient and sustainable treatment technologies, while also exposing the gaps that separate laboratory performance from practical deployment. Ferrite-based photocatalysts, particularly cerium-substituted Mn–Zn ferrites and alkaline earth ferrites, emerge as highly promising materials, achieving degradation efficiencies exceeding 92–97% under visible-light irradiation with the added advantage of magnetic recoverability [7, 8]. Heterostructure photocatalysts combining complementary materials, such as TiO_2–graphene oxide and CS–BiOCl/ZnO nanocomposites, demonstrate that rational material design can overcome the limitations of single-component systems [11, 12]. The mechanistic understanding of Congo red degradation has advanced considerably, with clear evidence for the role of reactive oxygen species, particularly hydroxyl radicals and superoxide anions, in driving mineralization, and with growing recognition that the dominant reactive species is a material-specific outcome rather than a universal property [5, 9]. The synergistic effects of adsorption and photocatalysis contribute to overall removal efficiency, particularly in nanocomposite materials with high surface areas, although adsorption must be distinguished from genuine mineralization when evaluating performance.

Despite these advances, challenges remain in terms of visible-light utilization, charge carrier recombination, long-term stability, and scalability. Several of the highest-

© Ariston Publications 2026. All rights reserved.

performing systems reported here still require UV activation, and reusability data over multiple cycles remain scarce for most materials. Future research should focus on developing multifunctional photocatalysts that combine high visible-light activity, magnetic recoverability, and excellent stability, while also addressing economic and practical considerations for industrial implementation. The field of photocatalytic degradation of Congo red and other azo dyes continues to evolve rapidly, with innovations in material design, synthesis methods, and mechanistic understanding. With continued research and development, photocatalytic technology holds genuine promise for addressing the global challenge of dye-contaminated wastewater and contributing to sustainable water resource management.

DECLARATIONS

Ethical Approval

We affirm that this manuscript is an original work, has not been previously published, and is not currently under consideration for publication in any other journal or conference proceedings. All authors have reviewed and approved the manuscript, and the order of authorship has been mutually agreed upon.

Funding

No funding.

Availability of data and material

All of the data obtained or analyzed during this study is included in the report that was submitted.

Conflicts of Interest

The authors declare that they have no financial or personal interests that could have influenced the research and findings presented in this paper. The authors alone are responsible for the content and writing of this article.

Authors' contributions

All authors contributed equally to this work,

REFERENCE

[1] Oladoye, P.O., Bamigboye, M.O., Ogunbiyi, O.D. and Akano, M.T., **2022**. Toxicity and decontamination strategies of Congo red dye. *Groundwater for Sustainable Development*, *19*, p.100844. https://doi.org/10.1016/j.gsd.2022.100844.

[2] Yakupova, E.I., Bobyleva, L.G., Vikhlyantsev, I.M. and Bobylev, A.G., **2019**. Congo Red and amyloids: history and relationship. *Bioscience reports*, *39*(1), p.BSR20181415. https://doi.org/10.1042/BSR20181415

[3] Rafatullah, M., Sulaiman, O., Hashim, R. and Ahmad, A., **2010**. Adsorption of methylene blue on low-cost adsorbents: a review. *Journal of hazardous materials*, *177*(1-3), pp.70-80. https://doi.org/10.1016/j.jhazmat.2009.12.047

[4] Quintanilla-Villanueva, G.E., Sicardi-Segade, A., Luna-Moreno, D., Núñez-Salas, R.E., Villarreal-Chiu, J.F. and Rodríguez-Delgado, M.M., **2025**. Recent advances in Congo red degradation by TiO2-based photocatalysts under visible light. *Catalysts*, *15*(1), p.84. https://www.mdpi.com/2073-4344/15/1/84

[5] Jasrotia, R., Jaswal, N., Prakash, J., Kit, C.C., Singh, J. and Kandwal, A., **2024**. Photocatalytic application of magnesium spinel ferrite in wastewater remediation: a review. *Journal of Magnesium and Alloys*, *12*(2), pp.490-505. https://doi.org/10.1016/j.jma.2024.02.006

[6] Chate, V.R., Desai, V.G.M., Dodagoudar, G.R., Guimarães, J.R. and Kulkarni, R.M., **2022**. Development of a novel photocatalyst: titania nanostructure bunches decorated on graphene oxide for enhanced photocatalytic efficiency. *Materials Research Bulletin*, *146*, p.111601. https://doi.org/10.1016/J.MATERRESBULL.2021.111601

[7] Ullah, I., Haider, A., Khalid, N., Ali, S., Ahmed, S., Khan, Y., Ahmed, N. and Zubair, M., **2018**. Tuning the band gap of TiO2 by tungsten doping for efficient UV and visible photodegradation of Congo red dye. *Spectrochimica Acta Part A: Molecular and Biomolecular Spectroscopy*, *204*, pp.150-157. https://doi.org/10.1016/j.saa.2018.06.046

[8] Khairol, N.F. and Sapawe, N., **2018**. Electrosynthesis of ZnO nanoparticles deposited onto egg shell for degradation of Congo red. *Materials Today: Proceedings*, *5*(10), pp.21936-21939. https://doi.org/10.1016/j.matpr.2018.07.053

[9] Sangon, S., Hunt, A.J., Ngernyen, Y., Youngme, S. and Supanchaiyamat, N., **2021**. Rice straw-derived highly mesoporous carbon-zinc oxide nanocomposites as high performance photocatalytic adsorbents for toxic dyes. *Journal of Cleaner Production*, *318*, p.128583. https://doi.org/10.1016/j.jclepro.2021.128583

[10] Michel, C.R. and Martínez-Preciado, A.H., **2023**. Adsorption and photocatalytic degradation of Congo red and malachite green by nanostructured Y2O3 synthesized by the coprecipitation method. *Open*

 © Ariston Publications 2026. All rights reserved.

Ceramics, *13*, p.100336. https://doi.org/10.1016/j.oceram.2023.100336

[11] Kerli, S., Soğuksu, A.K. and Kavgacı, M., **2020**. Production of nickel oxide nanostructure particles and their photocatalytic degradation of different organic dye. *International Journal of Modern Physics B*, *34*(09), p.2050081. https://doi.org/10.1142/S0217979220500812

[12] Vijayaraghavan, T., Suriyaraj, S.P., Selvakumar, R., Venkateswaran, R. and Ashok, A., **2016**. Rapid and efficient visible light photocatalytic dye degradation using AFe2O4 (A= Ba, Ca and Sr) complex oxides. *Materials Science and Engineering: B*, *210*, pp.43-50. https://doi.org/10.1016/j.mseb.2016.04.005

[13] Dinesh, A., Raja, K.K., Manikandan, A., Almessiere, M.A., Slimani, Y., Baykal, A., Alorfi, H.S., Hussein, M.A. and Khan, A., **2022**. Sol–gel combustion synthesis and photocatalytic dye degradation studies of rare earth element Ce substituted Mn–Zn ferrite nanoparticles. *Journal of Materials Research and Technology*, *18*, pp.5280-5289. https://doi.org/10.1016/j.jmrt.2022.04.121

[14] Ramadoss, G., Suriyaraj, S.P., Sivaramakrishnan, R., Pugazhendhi, A. and Rajendran, S., **2021**. Mesoporous ferromagnetic manganese ferrite nanoparticles for enhanced visible light mineralization of azoic dye into nontoxic by-products. *Science of the Total Environment*, *765*, p.142707. https://doi.org/10.1016/j.scitotenv.2020.142707

[15] Riyanti, F., Nurhidayah, N., Yuliasari, N. and Hariani, P.L., **2023**. MgFe2O4 magnetic catalyst for photocatalytic degradation of Congo red dye in aqueous solution under visible light irradiation. *Environ Nat Resour J*, *21*(4), pp.322-332. https://doi.org/10.32526/ennrj/21/20230002

[16] Zhang, E., Wang, L., Zhang, B., Xie, Y. and Wang, G., **2019**. Shape-dependent photocatalytic performance of SnFe2O4 nanocrystals synthesized by hydrothermal method. *Journal of Sol-Gel Science and Technology*, *89*(2), pp.355-360. https://doi.org/10.1007/s10971-018-4868-7

[17] Patel, M., Patel, M.H. and Sumesh, C.K., **2020**, May. Visible light enhanced photocatalytic performance of WS2 catalyst for the degradation of ternary dye mixture. In *AIP Conference Proceedings* (Vol. 2220, No. 1, p. 020047). AIP Publishing LLC. https://doi.org/10.1063/5.0001154

[18] Khatri, M., Gupta, A., Gyawali, K., Adhikari, A., Koirala, A.R. and Parajuli, N., **2022**. Photocatalytic degradation of dyes using synthesized δ-MnO2 nanostructures. *Chemical Data Collections*, *39*, p.100854. https://doi.org/10.1016/j.cdc.2022.100854

[19] Princy, S.S.J., Hentry, C., Alodaini, H.A., Hatamleh, A.A., Arokiyaraj, S. and Bindhu, M.R., **2023**. Hibiscus cannabinus seeds assisted spherical silver nanoparticles and its antibacterial and photocatalytic applications. *Chemical Physics Impact*, *6*, p.100192. https://doi.org/10.1016/j.chphi.2023.100192

[20] Chowdhury, A.P., Anantharaju, K.S., Keshavamurthy, K. and Rokhum, S.L., **2023**. Recent advances in efficient photocatalytic degradation approaches for azo dyes. *Journal of Chemistry*, *2023*(1), p.9780955. https://doi.org/10.1155/2023/9780955

[21] Ayub, A., Kim, B., Lim, Y., Devarayapalli, K.C., Kim, G. and Lee, D.S., **2023**. Hydrothermal synthesis of cobalt ferrite-functionalized Ti3C2Tx MXene for the degradation of Congo red via peroxymonosulfate activation system. *Journal of Alloys and Compounds*, *963*, p.171294. https://doi.org/10.1016/j.jallcom.2023.171294

[22] Al Naqeeb, N., **2026**. Pollution Control of Azo Dye–Contaminated Water Using TiO2/CNT/ZnCo2O4 Nanocomposite under Visible-Light Photocatalysis. *Journal of Nanostructures*, *16*(1), pp.978-987. https://doi.org/10.22052/JNS.2026.01.087

[23] Boulahbel, H., Benamira, M., Bouremmad, F., Ahmia, N., Kiamouche, S., Lahmar, H., Souici, A. and Trari, M., **2023**. Enhanced photodegradation of Congo red dye under sunlight irradiation by pn NiFe2O4/TiO2 heterostructure. *Inorganic Chemistry Communications*, *154*, p.110921. https://doi.org/10.1016/j.inoche.2023.110921

[24] Yadav, P., Dhariwal, N., Kumari, M., Kumar, V. and Thakur, O.P., **2023**. Enhanced degradation of Congo-red dye by Cr3+ doped α-Fe2O3 nano-particles under sunlight and industrial wastewater treatment. *Chemosphere*, *343*, p.140208. https://doi.org/10.1016/j.chemosphere.2023.140208

[25] Sudarsan, S., Anandkumar, M. and Trofimov, E.A., **2024**. Synthesis and characterization of copper ferrite nanocomposite from discarded printed circuit boards as an effective photocatalyst for Congo red dye degradation. *Journal of Industrial and Engineering Chemistry*, *131*, pp.208-220. https://doi.org/10.1016/j.jiec.2023.10.020

[26] Wahyuni, E.T., Lestari, N.D., Cinjana, I.R., Annur, S., Natsir, T.A. and Mudasir, M., **2023**. Doping TiO2 with Fe from iron rusty waste for enhancing its activity under

© Ariston Publications 2026. All rights reserved.

visible light in the Congo red dye photodegradation. *Journal of Engineering and Applied Science*, *70*(1), p.9. https://doi.org/10.1186/s44147-023-00178-9

[27] Movahedi, M., Mahjoub, A.R. and Janitabar-Darzi, S., **2009**. Photodegradation of Congo red in aqueous solution on ZnO as an alternative catalyst to TiO2. *Journal of the Iranian Chemical Society*, *6*(3), pp.570-577. https://doi.org/10.1007/BF03246536

[28] Hua, Z., Pan, Y. and Hong, Q., **2023**. Adsorption of Congo red dye in water by orange peel biochar modified with CTAB. *RSC advances*, *13*(18), pp.12502-12508. https://doi.org/10.1039/d3ra01444d

[29] Far, B.F., Naimi-Jamal, M.R., Jahanbakhshi, M., Khalafvandi, S.A., Alian, M. and Jahromi, D.R., **2024**. Decontamination of Congo red dye from aqueous solution using nanoclay/chitosan-graft-gelatin nanocomposite hydrogel. *Journal of Molecular Liquids*, *395*, p.123839. https://doi.org/10.1016/j.molliq.2023.123839

[30] Djelloul, A., Boutaleb, N., Ezzat, A.O., Sabantina, L., Abd-Elkader, O.H., Alkoudsi, B.D., Hamadouche, M. and Benyoucef, A., **2024**. Polyaniline–modified metal oxides adsorbents for the application in the Congo red dye adsorption. *Colloids and Surfaces A: Physicochemical and Engineering Aspects*, *703*, p.135266. https://doi.org/10.1016/j.colsurfa.2024.135266

[31] Alihassan, M.F.P. and Fawaz, M., **2023**. Design and synthesis of heteroatom modified highly crystalline carbon nitrides for energy storage and conversion applications.

[32] Alharbi, S.E., Zarewa, M.U. and Saleh, T.A., **2025**. Integrated adsorption–electrocoagulation for dyes removal using solid petcoke-derived activated carbon coupled with predictive machine learning models. *Diamond and Related Materials*, p.112825. https://doi.org/10.1016/j.diamond.2025.112825

[33] Choudhary, M., De, A. and Mishra, S., **2025**. Cellulose and metal–organic frameworks (MOFs): synergistic strategies for developing high-performance cellulose/MOFs composites. *Cellulose*, *32*(12), pp.6891-6933. https://doi.org/10.1007/s10570-025-06659-9

[34] Liu, L., Ma, Y., Yang, W., Chen, C., Li, M., Lin, D. and Pan, Q., **2020**. Reusable ZIF-8@ chitosan sponge for the efficient and selective removal of congo red. *New Journal of Chemistry*, *44*(36), pp.15459-15466. https://doi.org/10.1039/d0nj02699a

[35] Asses, N., Ayed, L., Hkiri, N. and Hamdi, M., **2018**. Congo red decolorization and detoxification by Aspergillus niger: removal mechanisms and dye degradation pathway. *BioMed research international*, *2018*(1), p.3049686. https://doi.org/10.1155/2018/3049686

[36] Akhter, M., Amin, M.K., Dhar, P.K., Dey, S.K., Hossain, M.S. and Dutta, S.K., **2024**. Fabrication of rare-earth cerium-doped nickel–copper ferrite as a promising photo-catalyst for congo red-containing wastewater treatment. *RSC advances*, *14*(40), pp.29083-29098. https://doi.org/10.1039/d4ra04334k

[37] Himanshi, Makasana, J., Ganesan, S., Lal, B., Naidu, K.S., Ahmed, J., Prakash, J., Verma, A., Lakshmaiya, N., Jasrotia, R. and Yong, X., **2025**. Insights into the enhanced photocatalytic degradation of congo red using advanced BaDyxFe12− xO19 catalytic hexamaterials. *Scientific Reports*, *15*(1), p.8978. https://doi.org/10.1038/s41598-025-92145-y

[38] Alqassem, B., Banat, F., Palmisano, G. and Haija, M.A., **2024**. Emerging trends of ferrite-based nanomaterials as photocatalysts for environmental remediation: A review and synthetic perspective. *Sustainable Materials and Technologies*, *40*, p.e00961. https://doi.org/10.1016/j.susmat.2024.e00961

[39] Wang, J., Wang, R., Zhang, Z., Chen, R. and Yang, J., **2026**. Recyclable magnetic g-C3N4@ NiFe0. 5Nd1. 5O4 nanosheets for enhanced removal of azo dyes: synergizing adsorption and visible-light photocatalysis. *Separation and Purification Technology*, p.138610. https://doi.org/10.1016/j.seppur.2026.138610

[40] Lestari, D., Masriah, I., Sari, J.N. and Daulay, A., **2026**. Recent Advances In Metal Co-Doped TiO_2 Photocatalysts For Enhanced Dye Degradation: A Systematic Review. *Moroccan Journal of Chemistry*, *14*(2), pp.486-507.

[41] Ayadi, I., Souissi, Y., Jlassi, I., Peixoto, F. and Mnif, W., **2016**. Chemical synonyms, molecular structure and toxicological risk assessment of synthetic textile dyes: a critical review. *J. Dev. Drugs*, *5*(2).

[42] Yakupova, E.I., Bobyleva, L.G., Vikhlyantsev, I.M. and Bobylev, A.G., **2018**. Congo Red and amyloids: history and relationship. *Bioscience Reports*, *20181415*, pp.10-1042. http://dx.doi.org/10.1042/BSR20181415

[43] Kennelly, J.C., Hertzog, P.J. and Martin, C.N., **1982**. The release of 4, 4′-diaminobiphenyls from azodyes in the rat. *Carcinogenesis*, *3*(8), pp.947-951. https://doi.org/10.1093/carcin/3.8.947

 © Ariston Publications 2026. All rights reserved.

[44] Saini, R. and Choudhary, K., **2025**. Toxic potential of azo dyes: A broader understanding. In *Hazardous chemicals* (pp. 469-481). Academic Press. https://doi.org/10.1016/B978-0-323-95235-4.00039-6

[45] Bafana, A., Jain, M., Agrawal, G. and Chakrabarti, T., **2009**. Bacterial reduction in genotoxicity of Direct Red 28 dye. *Chemosphere*, *74*(10), pp.1404-1406. https://doi.org/10.1016/j.chemosphere.2008.11.043

[46] Hernández-Zamora, M., Perales-Vela, H.V., Flores-Ortíz, C.M. and Cañizares-Villanueva, R.O., **2014**. Physiological and biochemical responses of Chlorella vulgaris to Congo red. *Ecotoxicology and Environmental Safety*, *108*, pp.72-77. https://doi.org/10.1016/j.ecoenv.2014.05.030

[47] Hernández-Zamora, M. and Martínez-Jerónimo, F., **2019**. Congo red dye diversely affects organisms of different trophic levels: a comparative study with microalgae, cladocerans, and zebrafish embryos. *Environmental Science and Pollution Research*, *26*(12), pp.11743-11755. https://doi.org/10.1007/s11356-019-04589-

[48] Raval, N.P., Shah, P.U. and Shah, N.K., **2016**. Adsorptive amputation of hazardous azo dye Congo red from wastewater: a critical review. *Environmental Science and Pollution Research*, *23*(15), pp.14810-14853. https://doi.org/10.1007/s11356-016-6970-0

[49] Reid, T.M., Morton, K.C., Wang, C.Y. and King, C.M., **1983**. Conversion of Congo red and 2-azoxyfluorene to mutagens following in vitro reduction by whole-cell rat cecal bacteria. *Mutation Research/Genetic Toxicology*, *117*(1-2), pp.105-112. https://doi.org/10.1016/0165-1218(83)90157-X

[50] Aounallah, F., Hkiri, N., Fouzai, K., Elaoud, A., Ayed, L. and Asses, N., **2024**. Biodegradation pathway of congo red azo dye by Geotrichum candidum and toxicity assessment of metabolites. *Catalysis Letters*, *154*(11), pp.6064-6079. https://doi.org/10.1007/s10562-024-04777-w

[51] Linsebigler, A.L., Lu, G. and Yates Jr, J.T., **1995**. Photocatalysis on TiO2 surfaces: principles, mechanisms, and selected results. *Chemical reviews*, *95*(3), pp.735-758. https://doi.org/10.1021/cr00035a013

[52] Hoffmann, M.R., Martin, S.T., Choi, W. and Bahnemann, D.W., **1995**. Environmental applications of semiconductor photocatalysis. *Chemical reviews*, *95*(1), pp.69-96. https://doi.org/10.1021/cr00033a004

[53] Fujishima, A., Zhang, X. and Tryk, D.A., **2008**. TiO2 photocatalysis and related surface phenomena. *Surface science reports*, *63*(12), pp.515-582. https://doi.org/10.1016/j.surfrep.2008.10.001

[54] Kumar, S.G. and Devi, L.G., **2011**. Review on modified TiO2 photocatalysis under UV/visible light: selected results and related mechanisms on interfacial charge carrier transfer dynamics. *The Journal of physical chemistry A*, *115*(46), pp.13211-13241. https://doi.org/10.1021/jp204364a

[55] Kong, M., Li, Y., Chen, X., Tian, T., Fang, P., Zheng, F. and Zhao, X., **2011**. Tuning the relative concentration ratio of bulk defects to surface defects in TiO2 nanocrystals leads to high photocatalytic efficiency. *Journal of the American Chemical Society*, *133*(41), pp.16414-16417. https://doi.org/10.1021/ja207826q

[56] Priyadarshini, U., Priya, Y.N. and Neelancherry, R., **2026**. Solar photocatalytic degradation of congo red from aqueous phase using modified ZnO/graphite carbon nitride nanocomposites. *Journal of Water Process Engineering*, *83*, p.109669. https://doi.org/10.1016/j.jwpe.2026.109669

[57] Schneider, J., Matsuoka, M., Takeuchi, M., Zhang, J., Horiuchi, Y., Anpo, M. and Bahnemann, D.W., **2014**. Understanding TiO2 photocatalysis: mechanisms and materials. *Chemical reviews*, *114*(19), pp.9919-9986. https://doi.org/10.1021/cr5001892

[58] Assem, B., Althobaiti, I.O. and Almulaiky, Y.Q., **2026**. Synergistic and Magnetically Recoverable NiFe2O4–MWCNT–CA Nanocomposites for Efficient UV-Driven Photodegradation of Organic Pollutants. *Catalysts*, *16*(3), p.262. https://doi.org/10.3390/catal16030262

[59] Galloni, M.G., Fabbrizio, V., Nasirova, G., Falletta, E., Giordana, A., Cerrato, G. and Bianchi, C.L., **2026**. From Selective Adsorption to Photocatalytic Removal: Complementary Cobalt Oxides for Pollutant-Oriented Treatment of Dye Mixtures. *Catalysts*, *16*(10), p.885. https://doi.org/10.3390/catal16100885.

© Ariston Publications 2026. All rights reserved.